GEOPHYSICS, VOL. 54, NO. 7 (JULY 1989); P. 872–888, 11 FIGS., 1 TABLE.

Depth of investigation in electromagnetic sounding methods

Brian R. Spies*

ABSTRACT

The time or frequency at which the electromagnetic (EM) response of a buried inhomogeneity can first be measured is determined by its depth of burial and the average conductivity of the overlying section; it is relatively independent of the type of source or receiver and their separation. The ability to make measurements at this time or frequency, however, depends on the sensitivity and accuracy of the instrumentation, the signal strength, and the ambient noise level. These factors affect different EM sounding systems in surprisingly different ways.

For the magnetotelluric (MT) method, it is possible to detect a buried half-space under about 1.5 skin depths of overburden. The maximum depth of investigation is virtually unbounded because of high signal strengths at low frequencies. Transient electromagnetic (TEM) soundings, on the other hand, have a limited depth of penetration, but are less affected by static shift errors. For TEM, a buried inhomogeneity can be detected under about one diffusion depth of overburden. For conventional near-zone sounding in which induced voltage is measured (impulse response), the depth of investigation is proportional to the 1/5 power of the source moment and ground resistivity. By contrast, if the receiver is a magnetometer (step response system), the depth of investigation is proportional to the 1/3 power of source moment and is no longer a function of resistivity. Magnetic-field measurements may, therefore, be superior for exploration in conductive areas such as sedimentary basins. Far-zone, or long-offset, TEM soundings are traditionally used for deep exploration. The depth of investigation for a voltage receiver is proportional to the 1/4 power of source moment and resistivity and is inversely proportional to the source-receiver separation. Magnetic-field measurements are difficult to make at long offsets because instrumental accuracy limits the measurement of the very slow decay of the magnetic field.

Frequency-domain controlled-source systems are ideally suited for sounding at the very shallow depths needed for engineering, archaeological, and groundwater applications because of the relative ease of extending the measurements to arbitrarily high frequencies, and also because geometric soundings can be made at low induction numbers.

INTRODUCTION

Estimation of the depth of investigation is crucial for both the design and interpretation of electromagnetic (EM) sounding experiments. Most geophysicists know that the basic parameters which control the depth of investigation include transmitter moment, noise levels, and earth resistivity; but the specific relationships of these parameters to the depth of investigation achieved are sometimes poorly understood. Survey design based on heuristic considerations or intuition can either fail to meet the geologic objectives or result in unnecessary expense. The purpose of this paper is to derive simple rules-of-thumb that can be used by the exploration geophysicist to calculate the depth of investigation for EM depth sounding methods commonly used.

EM sounding is widely used in petroleum, mineral, groundwater, and geothermal exploration and includes controlled-source techniques (both frequency- and time-domain) and natural-source techniques such as magnetotellurics. An overview of applications, methodology, and case histories for controlled-source techniques is given by Spies and Frischknecht (1989), and for magnetotellurics by Vozoff (1989). The techniques used most widely for geophysical sounding are the magnetotelluric (MT) and time-domain or

Based in part on a paper presented at the 53rd Annual International Meeting, Society of Exploration Geophysicists. Manuscript received by the Editor May 13, 1988; revised manuscript received January 18, 1989.
*ARCO Oil and Gas Company, 2300 W. Plano Parkway, Plano, TX 75075.

transient electromagnetic (TEM) methods, which together comprise approximately 76 percent of EM surveys (by dollars spent) in the Western world (Montgomery, 1987). Magnetotellurics is used mainly for structural mapping of basins, especially those covered with resistive volcanic or overthrust material, whereas TEM is used for shallower sounding and stratigraphic applications. Frequency-domain electromagnetic (FEM) soundings are used mainly for shallow engineering, archeological, environmental, and groundwater studies.

It is sometimes difficult to choose the optimal EM sounding method, particularly since advances in instrumentation have widened the depth range beyond that which was possible in the past. Having chosen the method, the design of the survey must be such that the desired depth of investigation can be achieved. In some geologic environments there may be advantages in using a combination of techniques. For example, corrections for MT static shifts based on TEM measurements (Andrieux and Wightman, 1984; Sternberg et al., 1988) depend on an adequate overlap in the depths of investigation of the two techniques.

In this paper, I relate the depth of investigation to the physics of EM diffusion, instrument sensitivity, and noise levels for the MT and TEM methods. Rules-of-thumb are derived which can be used by the exploration geophysicist both to design a field survey and to choose the optimum field parameters so that the EM sounding covers the desired range of depths.

THEORETICAL BACKGROUND

To understand which parameters affect the depth of penetration, it is helpful to consider the diffusion and attenuation of EM fields within the earth. For a uniform earth and spatially one-dimensional (1-D) (plane-wave) fields the orthogonal electric- and magnetic-field components in the earth are (Nabighian and Macnae 1989)

$$E_x(z, t) = E_{x_0} e^{-iz/\delta} e^{-z/\delta} e^{i\omega t} \tag{1a}$$

and

$$H_y(z, t) = E_{x_0} \sqrt{\frac{\sigma}{\mu_0 \omega}}\, e^{-i\pi/4} e^{-iz/\delta} e^{-z/\delta} e^{i\omega t}, \tag{1b}$$

where E_{x_0} is the field at the surface, and

$$\delta_{FD} = \sqrt{\frac{2}{\sigma \mu_0 \omega}} \tag{2}$$

is the frequency-domain (FD) skin depth. It is assumed that conductivity σ and magnetic permeability μ_0 are frequency-independent and that displacement currents can be ignored. As can be seen from these equations, the depth $z = \delta$ is the depth at which the EM field is reduced to $1/e$, or 37 percent, of its value at the surface, while the phase is rotated by one radian.

The time-domain analogs to these equations are given by Wait (1969) and Nabighian and Macnae (1989). For a step-function excitation of magnitude h_0 established at time $t = 0$, the transient fields are

$$e_x(z, t) = \frac{2h_0}{\sigma} \frac{1}{\sqrt{2\pi}} \sqrt{\frac{\sigma\mu_0}{2t}}\, e^{-(\sigma\mu_0/2t)(z^2/2)}, \tag{3a}$$

and

$$h_y(z, t) = h_0 \operatorname{erfc}\left(\sqrt{\frac{\sigma\mu_0}{2t}} \frac{z}{\sqrt{2}}\right), \tag{3b}$$

where erfc is the complementary error function. For a fixed time t, the variation of $e_x(z, t)$ and $h_y(z, t)$ with depth is similar to the normal density and normal distribution function with zero mean and variance $\sqrt{2t/\sigma\mu_0}$. By keeping z fixed in equation (3a) and equating to zero the derivative of $e_x(z, t)$ with respect to time, the maximum transient electric field at any time t can be shown to be located at a depth of

$$\delta_{TD} = \sqrt{\frac{2t}{\sigma\mu_0}}, \tag{4}$$

where the quantity δ_{TD} is the time-domain diffusion depth. The similarity between the expressions for diffusion depth [equation (4)] and skin depth [equation (2)] is remarkable; the depths are proportional to $1/\sqrt{\omega}$ in the frequency domain, and $\sqrt{t}$ in the time domain. As a function of time, the time-domain diffusion depth travels downward with a velocity given by

$$v = \frac{1}{\sqrt{2\sigma\mu_0 t}}.$$

The subsurface pattern of the diffusion currents is an expanding, attenuating image of the source geometry, and is most easily visualized in the time domain. "Snapshot" images of the electric-field strength in a homogeneous earth are given by Nabighian and Macnae (1989) for a plane-wave source, by Oristaglio (1982) for a line source, by Lewis and Lee (1978), Hoversten and Morrison (1982), and Newman et al. (1989) for a loop source, and by Gunderson et al. (1986) for a grounded wire and infinite line source.

The terms "skin depth" and "depth of penetration" are often assumed to be synonymous in elementary textbooks, although in practice it is necessary to distinguish between these two terms. Theoretically the EM fields at any frequency or time are present at all depths, albeit at vanishingly small values. The *practical* depth of investigation from the geophysical standpoint depends on such factors as the sensitivity and accuracy of the instrumentation, the complexity of the geologic section, and the ambient or inherent noise levels. In an ideal geologic environment, the practical depth of investigation may be several skin depths, whereas in geologically complex or noisy areas, and for certain EM sounding systems, it may be much less than one skin depth.

Most approximate 1-D interpretation schemes (e.g., Bostick, 1977) are based on a direct transformation of the data to a conductivity-depth section. The "effective depth of penetration" defined in these schemes is closely related to skin depth or diffusion depth (see Appendix A) and is controlled by the conductivity of the ground and the frequency (or time) of measurement which, together, determine the depth to which the induced currents have diffused.

The approach used in this paper is to find the highest frequency (or earliest time) at which a homogeneous half-

space buried beneath a uniform layer has a measurable effect on the observed response. It is argued that the expressions so derived are also valid for detection of 2-D and 3-D bodies at depth.

DETECTABILITY OF A BURIED HALF-SPACE

Magnetotelluric sounding

The factors affecting the depth of investigation can most easily be studied by considering the suite of two-layer Cagniard apparent resistivity and phase curves shown in Figure 1. The basic features of these curves are well-known: the response at high frequencies is dominated by the upper layer, while the underlying half-space dominates at low frequencies.

The "depth of investigation" is defined here as the maximum depth at which a buried half-space can be detected by a measurement system at a particular frequency. This depth is dependent on the conductivity contrast and the accuracy of the recording and processing system. Consider a system having a measurement accuracy of ±3 dB in the magnitude of E/H, which corresponds to an accuracy of ±6 dB in apparent resistivity. The response of a two-layer earth with a conductivity contrast of 2 lies inside the error bounds at all frequencies (shaded region in Figure 1). However, the response of the same model having a conductivity contrast of 5 is outside the error bounds when the overburden is less than 0.3 skin depths thick.

On the other hand, if the measurement accuracy were increased so that apparent resistivity could be measured to ±0.1 dB (i.e., approximately 1 percent), then the layering would be observable under two skin depths of overburden. Most interpreters, however, would not be confident in basing their interpretation on a small phase shift and the start of a small undershoot or overshoot in the apparent resistivity data (although their automated computer inversion programs may have no such qualms). An interpreter usually assigns a "comfort" or "confidence" factor based on typical, or best-case, data quality and system accuracy, and experience. I assume here that apparent resistivity can be measured with an accuracy of ±0.8 dB (approximately 10 percent), which would enable the detection of a buried half-space with a conductivity contrast of 10 under 1.5 skin depths of overburden. Examination of other curves based on alternative definitions of apparent resistivity (e.g., Spies and Eggers, 1986) supports this observation. Furthermore, Szarka and Fischer (1989), by analysis of the real and imaginary parts of the impedance, show that the final deviation of the phase curve from 45 degrees at $d/\delta = 1.5$ physically implies the final separation of the centers of the in-phase and out-of-phase current systems at depth d. Thus, a reasonable estimate for the depth of investigation for MT is taken to be approximately equal to 1.5 skin depths, or

$$z \approx 1.5\,\delta_{FD} = 1.5\sqrt{\frac{2}{\sigma_1\mu_0\omega}} = 750\sqrt{\frac{1}{\sigma_1 f}}. \qquad (5)$$

One method of estimating the contribution to the EM response from various depths is to calculate the Fréchet derivatives from the appropriate integral equation (e.g., Parker, 1977; Oldenburg, 1979; Chave, 1984; Edwards, 1988). The Fréchet derivatives give the sensitivity of the measurements to small local changes in conductivity, and the shape of the Fréchet kernel may be analyzed to obtain approximate penetration depths and the resolution intervals associated with any model and depth interval. By analysis of Fréchet derivatives for a plane-wave source, it is shown in Appendix B that 95 percent of the MT response from a homogeneous earth originates from depths of less than 1.5 skin depths.

Maximum depth of investigation.—There is no difficulty in extending an MT sounding to arbitrarily great depths, since the signal strength increases approximately in proportion to $1/f$. The maximum depth of investigation is not limited by system sensitivity or noise levels but depends only upon the measurement frequency and earth conductivity as described by equation (5). There are major differences in the analogous expressions for TEM sounding, as is shown in a later section.

Upper limit of investigation.—The ability to resolve *shallow* parts of the geoelectric section is limited by the

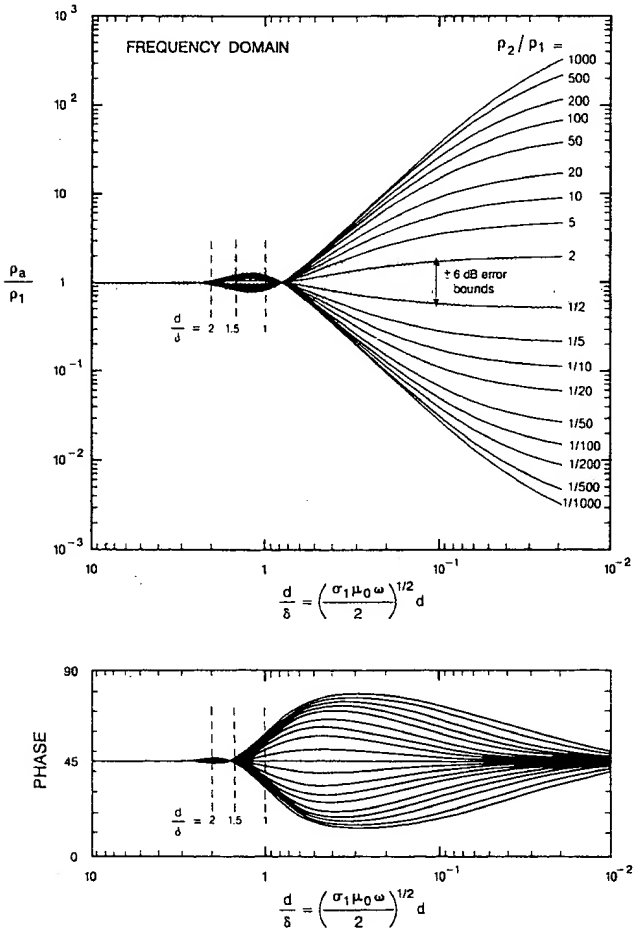

FIG. 1. MT Cagniard apparent resistivity and phase curves for a two-layer earth. The horizontal axis is the upper layer thickness expressed in skin depths. Dashed vertical lines superimposed on the figure correspond to values of 1, 1.5, and 2 skin depths.

highest frequency of measurement (usually <100 Hz, but up to 15 kHz in some MT systems). From apparent resistivity or amplitude data, only the "average" conductivity σ_{av} of the geoelectric section lying above the penetration depth z_{min} calculated at this frequency can be determined. z_{min} can be considered the *minimum* resolvable depth obtainable in an MT sounding and is calculated by substituting σ_{av} for σ_1 in equation (5). The depth at which conductivity variations can be investigated is a function of both resistivity and frequency and is shown in diagrammatic form in Figure 2.

It should be mentioned that if phase (or the derivative of amplitude) is available, then additional constraints can be placed on the conductivity structure above z_{min}. For example, Schmucker (1987) describes two extremal models with large resistivity contrasts where the top layer acts either as a nonconductor (h-model) or as a thin-sheet conductor (τ-model). For the h-model, the phase of the impedance $\phi(\omega)$ lies between 45 and 90 degrees, and for the limiting case of a perfectly resistive top layer of thickness h overlying a basal half-space, the MT response is given by $Z(\omega)/i\omega = h + (1 - i)\delta_2(\omega)/2$, where $\delta_2(\omega)$ is skin depth in the basal half-space. For the τ-model, the phase lies between 0 and 45 degrees, and the limiting model is that of a thin surface layer of conductance S overlying a half-space, for which the MT response is $i\omega/Z(\omega) = i\omega\mu_0 S + (1 + i)/\delta_2(\omega)$. If the phase is 45 degrees, the response reverts to that of a uniform half-space, with resistivity equal to the Cagniard apparent resistivity.

Depth of investigation in a multilayered earth.—The depth of investigation given by equation (5) can be extended to a multilayered earth by replacing σ_1 by the "effective" or "average" conductivity of the ground overlying the depth of investigation. The efficacy of using the effective or average conductivity is illustrated by numerous studies of the equivalence and nonuniqueness of multilayered earth models that have appeared in the inversion literature in the last two decades. In the case of imprecise observations (i.e., all those obtained in practice), individual inversion algorithms can yield very different solutions, and the data can be fit with a large variety of models. These range from the delta function D^+ models of Parker (1980), through simple layered models familiar to most geophysicists (Jupp and Vozoff, 1975; Nabetani and Rankin, 1969; Glenn et al., 1973; Larsen, 1981), to smoothly varying models (Glasko et al., 1972; Weidelt, 1972; Oldenburg, 1979; Oldenburg et al., 1984; Constable et al., 1987; Srnka and Crutchfield, 1987). Examples of vastly different models fitting an observed data set are given by Jones and Hutton (1979), Parker and Whaler (1981), Oldenburg et al. (1984), and Constable et al. (1987).

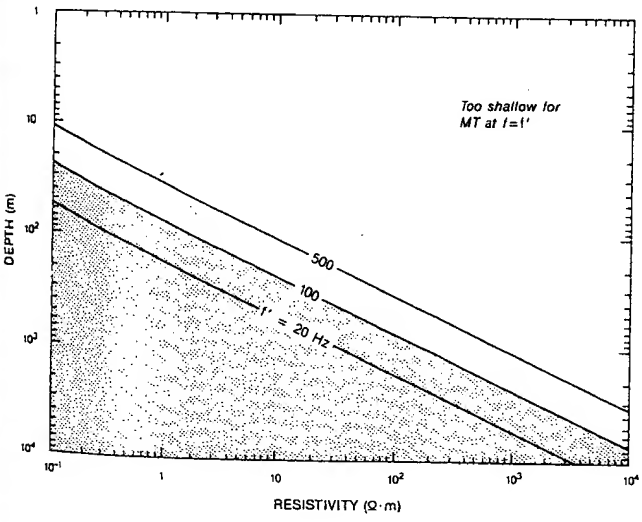

FIG. 2. Depth of investigation (shown shaded) attainable with an MT system with an upper frequency limit f'. At depths shallower than those given by the diagonal line [given by equation (5)], the response is controlled mainly by the integrated conductance of the overlying section; and the conductivity structure cannot be resolved.

Much more stable inversions are achieved if the solution is sought in terms of integrated or cumulative conductance down to depth z,

$$S(z) = \int_0^z \sigma(z)\, dz. \tag{6}$$

This result comes from the classic study of thin sheets by Price (1949) and has been used by numerous other workers, e.g., Schmucker (1970), Fullagar and Oldenburg (1984), and Macnae and Lamontagne (1987). Oldenburg (1983) and Weidelt (1985) discuss the issue of extremal bounds on integrated conductance estimates.

To estimate the depth of investigation in a multilayered earth section, the integrated conductance obtained from a conventional layered-earth inversion is first calculated as a function of depth z. The "average" or "effective" conductivity at each depth, given by

$$\sigma_{av}(z) = \frac{S(z)}{z} \tag{7}$$

(Jain, 1966), is also calculated. This process is continued at increasing depths until z reaches the same value as that obtained from equation (5) at the lowest measurement frequency, f_{min}. The value of z so obtained will be the maximum depth of investigation z_{max}. It should be stressed that even though the layered-earth linearized inversion may result in interpreted layers deeper than this value, their existence is not supported by the data. In addition, care must be taken that static shifts have not corrupted the inversion results. This is a particular problem with the MT method and is discussed in more detail in the "Discussion" section.

This relatively straightforward approach to calculating the depth of investigation can be tested against the rigorous but computationally formidable method described by Parker (1982). Using quadratic programming techniques, Parker shows that there is a "critical depth" below which the model conductivity can be chosen arbitrarily without degrading the goodness of fit of the data to the model. His critical depth is thus, in effect, the practical depth of investigation.

I tested a data set from a long-period MT experiment described by Parker and Whaler (1981) which had been inverted to a number of different model solutions including simple layered models, smooth models, and delta function D^+ models. Although the models were very different, their

integrated conductance-versus-depth functions were reasonably alike. One inversion result from Parker and Whaler's paper is shown in Figure 3a. The procedure used to calculate the maximum depth of investigation z_{max} follows that outlined above: first, the integrated conductance $S(z)$ and the average conductivity $\sigma_{av}(z)$ are calculated from equations (6) and (7); these are plotted in Figures 3a and 3b. Values of the apparent maximum depth $z_{max_a}(z)$ are then calculated for successive depths by substituting $f = f_{min}$ and $\sigma_1 = \sigma_{av}(z)$ into equation (5), i.e., $z_{max_a}(z) = 750\,[\sigma_{av}(z) f_{min}]^{-1/2}$.

The value of z for which $z = z_{max_a}$ is given by the intersection of the two lines in Figure 3c, and in this example equals 620 m. The certainty with which the depth of investigation can be estimated is determined by the angle subtended by these two lines. As can be seen from Figure 3c, $z_{max_a}(z)$ decreases rapidly when conductive layers are encountered and increases slowly in resistive layers.

The depth of investigation calculated with this procedure is within 10 percent of Parker and Whaler's estimate. Equally good estimates were obtained for other models in Parker and Whaler's paper, including smooth and delta-function models. In contrast to Parker and Whaler's technique, however, the approximate scheme suggested above is very simple to implement and easy to calculate.

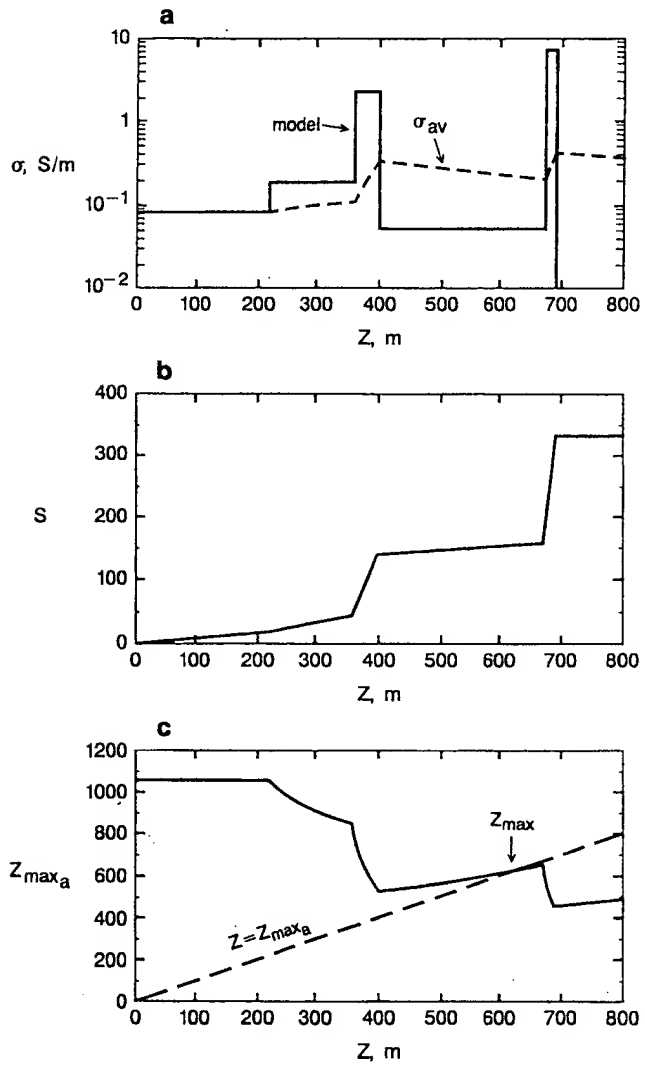

FIG. 3. Procedure for calculating the depth of investigation for a layered-earth model. (a) The model and its associated average conductivity $\sigma_{av}(z)$ calculated from the integrated conductance $S(z)$ shown in (b). (c) shows the apparent maximum depth of investigation $z_{max_a}(z)$ calculated from equation (5) at the lowest measurement frequency, using $\sigma_1 = \sigma_{av}(z)$. The maximum depth of investigation is the value for which $z = z_{max_a} = z_{max}$. (The model is adapted from Parker and Whaler, 1981.)

Transient electromagnetic sounding

A similar analysis can be applied to TEM data. In this case, the upper limit of depth of investigation is controlled by the earliest sample time of measurement (50 μs in many systems, but as early as 6 μs in some). Unlike the MT case, however, the lower limit is determined by the time at which the signal decays into noise. Two commonly used configurations are considered: the in-loop or central induction configuration in which a vertical-axis receiver is located at the center of a transmitter loop, and the wire-loop configuration which employs a grounded wire source.

Time of departure.—A suite of TEM magnetic-field and time-derivative (voltage) response curves for the in-loop configuration is shown in Figures 4 and 5. These data are for a step turnoff of current into a transmitter loop of radius a over a two-layer earth with upper layer thickness d. The vertical axis in these graphs is the measured response, either magnetic field $h_z = B_z/\mu_0$ or induced voltage dB_z/dt; this provides a more realistic estimate of resolution than does apparent conductivity, which is a nonlinear function. The horizontal axis is presented in two forms: the bottom axis is normalized time τ, and the top axis is the thickness of the upper layer expressed in diffusion depths, defined by equation (4). τ is a dimensionless quantity which reduces to time for a fixed geologic model.

Similar responses to these are obtained for the wire-loop configuration, with a grounded-wire source of length $d\ell$ separated from the vertical-axis receiver by a distance a, located on an axis perpendicular to the transmitter. The response for this geometry can be obtained by multiplying the in-loop response by $d\ell/2\pi a$ to adjust for source moment, noting that a is now the source-receiver separation. The ordinate becomes $V 2\pi\sigma a^4/Id\ell m$ for voltage response (Figure 4), and $h_z 2\pi a^2/Id\ell$ for magnetic-field response (Figure 5).

Consider first the two sets of curves for voltage response shown in Figure 4. Values of $a/d = 25$ represent "far-zone" soundings for which the loop size or source-receiver separation is much larger than the diffusion depth, and values of $a/d = 1$ are for "near-zone" soundings for which the loop size or source-receiver separation is less than the diffusion depth. As noted by Raiche and Spies (1981), Kauahikaua (1981), and Spies and Eggers (1986), the time at which the second layer is first detected (termed here the time of departure) is reasonably constant for all models. The depth of penetration depends *primarily on the sample time and not the loop size or source-receiver separation*. Changes in conductivity at depths greater than the "depth of penetration" impart a negligible change to the response at times

earlier than the time of departure. In most cases, the lower layer is evident at a normalized time

$$\tau = \frac{2t}{\sigma\mu_0 d^2} \approx 1. \tag{8}$$

Another way of expressing this is that the lower layer can be detected beneath an upper layer with thickness equal to the diffusion depth δ_{TD} as defined by equation (4).

The departure of the curves from the response of the top layer is more readily observed for some models than others. For example, the separation between the curves, and hence the detectability, increases with conductivity contrast. As with the MT case, the value chosen for d/δ or τ depends on the accuracy of measurement. For a 20 percent difference between curves with a conductivity contrast of 10, the departure point ranges from $\tau = 0.4$ to 4.0 for voltage measurements, and 0.7 to 6.0 for magnetic-field measurements. At $\tau = 1$, the difference between the curves ranges from 1 percent to 80 percent, depending on the model.

For the magnetic-field response shown in Figure 5, the separation between the far-zone ($a/d = 25$) curves is gradual; and it is difficult to choose an appropriate value for the time of departure because the magnetic-field response at early times, given by

$$h_z^e = \frac{I}{2a}\left(1 - \frac{6t}{\sigma\mu_0 a^2}\right), \tag{9}$$

decays linearly from the primary field value at $t = 0$. It is only when intermediate times are reached ($\tau \approx 10$ to 20) that the decay rate increases to more easily observed values. Although the separation between the curves at earlier times would be much greater if the data were displayed as apparent conductivity, it would not be possible in practice to measure with sufficient accuracy to make these values meaningful. In general, for near-zone and intermediate-zone sounding, a conductive layer is more easily detected at a given time than is a resistive layer. For far-zone sounding, conductive or resistive layers have similar sensitivities for voltage (dB/dt) measurements.

Sensitivity functions for the in-loop TEM response for both magnetic-field and voltage measurements are plotted in Figure 6. These were computed numerically by perturbing the conductivity of a thin layer in an otherwise uniform half-space. The thickness of the layer was set equal to one-tenth of its depth and its conductivity was twice that of the background. The function $\gamma(z)$ is the percentage change in measured response resulting from the conductivity perturbation. For the case of a thin resistive layer (having a conductivity contrast the reciprocal of that used for the conductive layer), the $\gamma(z)$ functions retain the same shape; but the amplitudes are reduced to one-half those shown and the signs are reversed. For near-zone sounding ($a/d < 1$), the maximum contribution originates from a depth of 0.45 diffusion depths for magnetic-field measurements and 0.35 diffusion depths for voltage measurements. As expected from inspection of Figure 4, the undershoot for the voltage response increases in magnitude as the a/d ratio increases. Approximately 10 percent of the response for near-zone sounding is obtained at values of $d/\delta > 1$, i.e., when the buried layer is overlain by one diffusion depth of overburden. This is true both for voltage and magnetic-field measurements, except for the magnetic-field far-zone case discussed earlier. In the following discussion, a value of $\tau = 1$

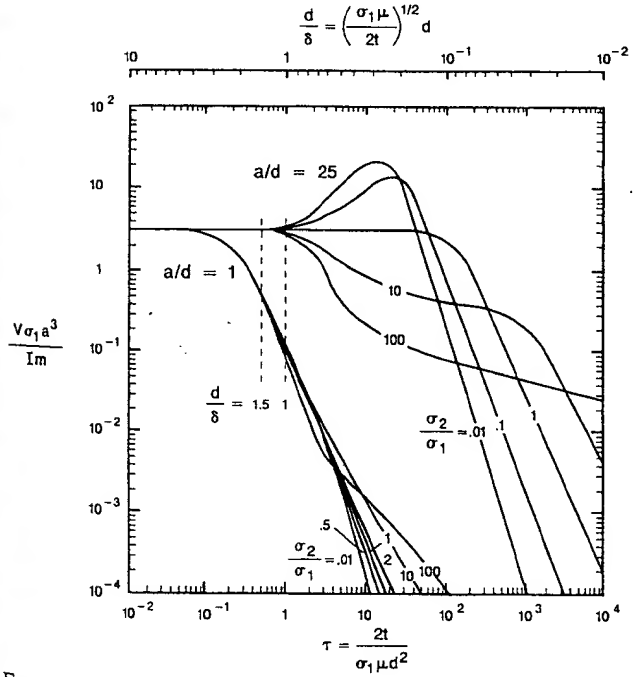

FIG. 4. TEM voltage response curves for a two-layer earth. The upper set of curves ($a/d = 25$) is for sounding in the far zone (long offset or large loop), and the lower set ($a/d = 1$) is for the near zone (small loop or short offset). The second layer is detectable under 1 diffusion depth of overburden (i.e., $d/\delta \approx 1$ and $\tau \approx 1$).

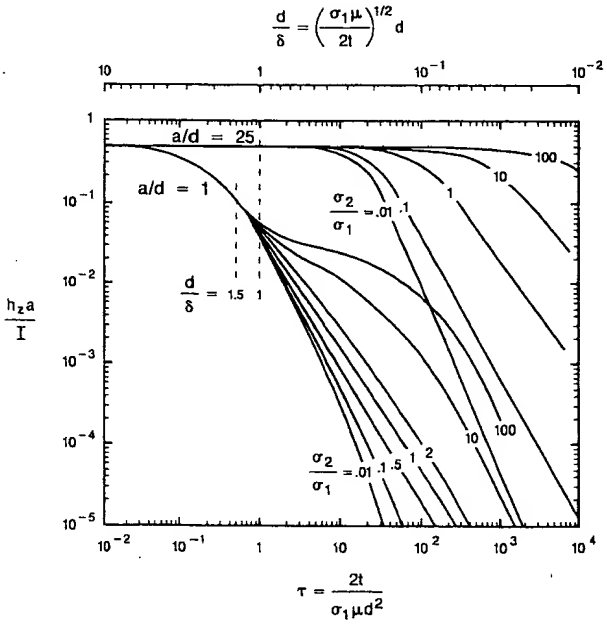

FIG. 5. TEM magnetic field response curves for a two-layer earth. The second layer is evident at $d/\delta \approx 1$ for the near zone ($a/d = 1$), but is difficult to discern in the far zone ($a/d = 25$) until much later in time.

is taken to be a reasonable value for the time of departure for all but far-zone magnetic-field measurements. As is shown below, this value can be modified to suit the preference of the reader without altering the main conclusions of the paper.

It is instructive to compare these curves with the corresponding sensitivity functions for magnetotellurics, which are displayed as dashed lines. The MT sensitivity functions are based on the measured $|E/H|$ values, not on apparent conductivity, in order to facilitate comparison with the TEM curves. The curve plotted on the top graph is the time-domain MT response (Kunetz, 1972), and the curve on the lower graph is the conventional frequency-domain response. Twenty-five percent of the time-domain MT response originates from $d/\delta > 1$ and 3 percent from $d/\delta > 1.5$. In the frequency domain, the respective numbers are 26 percent and 18 percent. Comparing the curves in Figure 6, it is evident that TEM near-zone sounding ($a/d \leq 1$) has the maximum sensitivity.

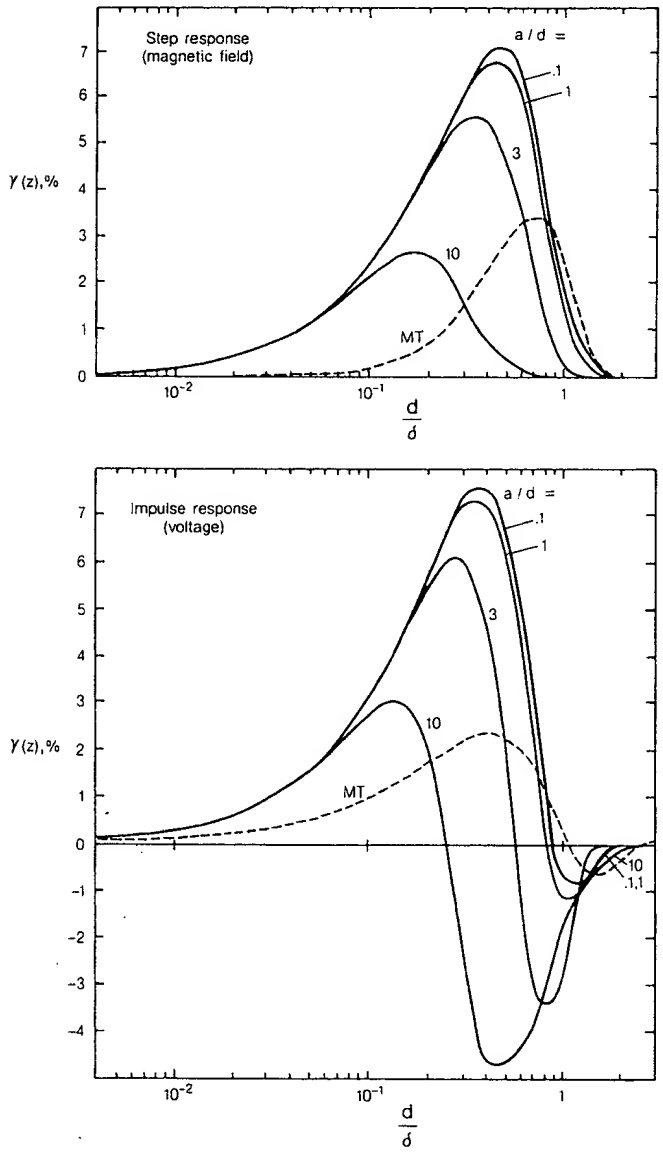

FIG. 6. Sensitivity functions for TEM, based on the response of a thin conductive layer at depth d, calculated for a magnetic-field receiver (top) and a voltage receiver (bottom). Corresponding MT sensitivity functions for $|E/H|$ measurements (dashed) are superimposed on the graphs. The basic features are similar to the TEM curves, but the amplitudes are lower.

Depth of investigation.—The practical limitation on the depth of investigation for TEM systems is determined by the time t' at which the signal decays to the noise level, the source moment, and earth resistivity. The time at which a buried layer can be first detected [t in equation (8)] is a function of the depth to the layer and the average resistivity of the overlying section. The two times t and t' can be equated to yield the thickness of overburden for which the TEM signal equals the noise level for any combination of source moment and earth resistivity. The thickness of overburden for which the signal equals the noise level is defined to be the maximum depth of investigation.

Noise sources not geologic in origin include geomagnetic micropulsations, spherics, cultural noise (power lines), wind noise, and instrumental or amplifier noise. The recorded noise is drastically reduced by time averaging (grouping the samples into time windows) and ensemble averaging (stacking repeated transients) and can be further reduced by noise prediction techniques (Spies, 1988). In most TEM systems the window width is a fraction α of the sample time t. Typically, field measurements are averaged for 15 minutes or so at each station in an attempt to achieve a reasonable noise level. The total number of samples averaged in the time window immediately preceding the next current pulse is equal to $T/2\alpha\Delta t$, where T is the total data acquisition time and Δt is the digitizing interval. Thus the total number of samples does not depend on the sample time t or the ground conductivity. In more conductive areas, the measured transient is longer and fewer transients are recorded in a given acquisition time, but the window width increases in such a way that the total number of averaged samples remains constant. For statistically independent white band-limited noise, the resultant noise level after averaging is independent of sample time, and the effective bandwidth BW is equal to $1/\alpha T$. Although in practice the observed noise spectrum is not white and the samples are not statistically independent, there is a large enough variability to make these assumptions reasonable for the analysis which follows, especially in the frequency range 0.1 Hz to 1.0 kHz applicable to deep TEM soundings. It is interesting to note that remote reference noise-cancellation schemes effectively whiten the resultant spectrum (Nichols et al., 1988).

The spectral shape and amplitude observed in practice can be highly variable and depend on such factors as geographic location and season (spherics are highest in the summer and at mid-latitudes), time of day, and weather conditions. I assume that estimates of the noise levels obtained after windowing, stacking, and other noise-reduction schemes are available from field measurements or published data for the survey area of interest. Typically, values obtained after 15 minutes of stacking range from 10^{-3} nT in winter to 2×10^{-4} nT in summer for magnetic-field measurements (denoted by η_B), and from 0.1 to 0.5 nV/m^2 in winter and 2 to 10 nV/m^2 in summer for voltage (dB/dt) measurements (denoted by η_v).

Near-zone sounding.—Near-zone, or short-offset, sounding refers to cases in which the loop size or source-receiver separation is less than the depth of investigation; the induction number $2t/\sigma\mu_0 a^2$ is greater than unity. The response of the buried layer is observed on the descending branch of the half-space curve (the so-called "late-time" region), as shown in Figures 4 and 5 ($a/d = 1$). The derivations which follow are for the in-loop configuration, but can also be used for the wire-loop configuration in slightly modified form.

(a) Magnetic field response.—The signal amplitude at times when the second layer is detected in near-zone sounding is given by the late-time asymptotic expression for a homogeneous half-space with conductivity σ for the upper layer,

$$h_z^{\ell} = \frac{I\sigma^{3/2}\mu_0^{3/2}a^2}{30\sqrt{\pi}t^{3/2}} \tag{10}$$

(Spies and Eggers, 1986). Equating the time term in equation (10) with the time of departure [equation (8)], it can be shown that

$$d \approx 0.26\left(\frac{IA}{h_z}\right)^{1/3}, \tag{11}$$

where A is the loop area and I is the transmitted current. Setting $B_z = \mu_0 h_z$ equal to the system noise level η_B,

$$d \approx 2.8 \times 10^{-3}\left(\frac{IA}{\eta_B}\right)^{1/3}. \tag{12}$$

For a typical noise level of 10^{-3} nT, this becomes

$$d \approx 28\,(IA)^{1/3}. \tag{13}$$

An example of the range of depths investigated with magnetic-field near-zone sounding is shown in Figure 7. The maximum depth is given by equation (12). The *minimum* depth is determined by the earliest sample time and is found by solving for d in equation (8). Above this depth only the integrated conductance for the overlying section can be determined.

(b) Voltage response.—Similarly, the late-time voltage (dB/dt) response for the in-loop configuration

$$V^{\ell} = \frac{I\sigma^{3/2}\mu_0^{5/2}a^2}{30\sqrt{\pi}t^{5/2}} \tag{14}$$

and equation (8) can be combined to obtain

$$d \approx 0.55\left(\frac{IA}{\sigma V}\right)^{1/5}. \tag{15}$$

As before, we can equate the response V with the noise level η_v to obtain

$$d \approx 0.55\left(\frac{IA}{\sigma\eta_v}\right)^{1/5}. \tag{16}$$

For a typical noise level η_v of 0.5 nV/m^2,

$$d \approx 40\left(\frac{IA}{\sigma}\right)^{1/5}. \tag{17}$$

These results are displayed graphically in Figure 8, using the same source parameters as Figure 7.

The most surprising result of these derivations is that, unlike the result obtained for voltage measurements [equation (15)], the depth of investigation obtained with magnetic-field measurements does not depend on the conductivity of the ground. This result appears at first to be counterintuitive. However, it can be seen from equation (10) that the dependence of magnetic-field response on time is the reciprocal of its dependence on conductivity, and thus, for any fixed value of h_z, an increase in conductivity is matched directly by a corresponding increase in sample time. Therefore, as long as the noise level is independent of time, the depth of investi-

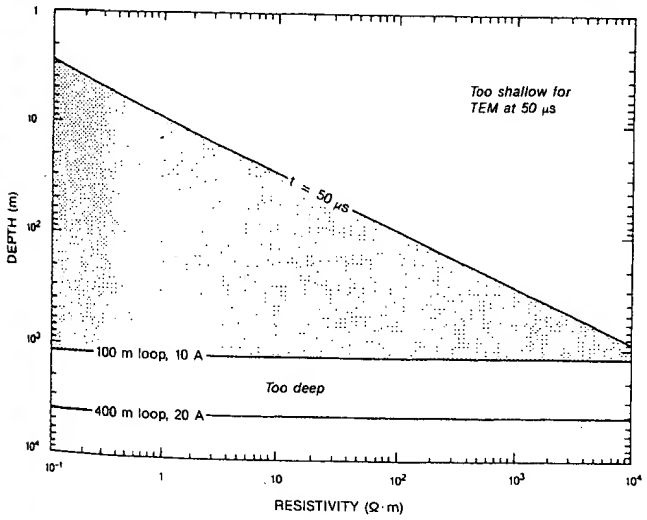

FIG. 7. Depth of investigation (shown shaded) attainable with a TEM system measuring magnetic field, assuming a noise level of 10^{-3} nT and loop parameters shown. The maximum depth [given by equation (12)] does not depend on conductivity. The minimum depth is given by equation (8).

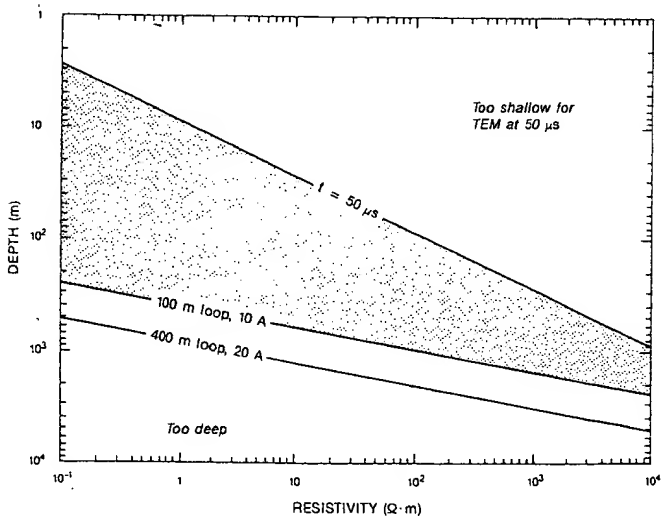

FIG. 8. Depth of investigation (shown shaded) attainable with a TEM system measuring voltage, assuming a noise level of 0.5 nV/m^2. The maximum depth [given by equation (16)] is proportional to the average resistivity of the overlying section, raised to the 1/5 power. The minimum depth is given by equation (8).

gation is independent of conductivity. For the voltage response [equation (14)], time and conductivity have different power-law dependencies.

The relationships given for depth of investigation in equations (12) and (16) exhibit different dependencies on source moment for magnetic-field and voltage response systems (1/3 and 1/5, respectively). Doubling the source moment increases the depth of exploration by 26 percent for magnetic-field measurements but only 15 percent for voltage measurements. In order to double the depth of exploration, it is necessary to increase the transmitter moment by factors of 8 and 32 for magnetic-field and voltage measurements, respectively. These formulas can also be used for the wire-loop configuration, by replacing the loop area A by $ad\ell/2$, where a is now the source-receiver separation and $d\ell$ is the dipole length.

Voltage measurements are superior for penetrating resistive areas, but magnetic-field measurements are superior for conductive areas. For the in-loop configuration, the earth conductivity σ for which both modes have identical depths of penetration can be derived by combining equations (12) and (16) to obtain

$$\sigma = \frac{3.1 \times 10^{11} \eta_B^{5/3}}{(IA)^{2/3} \eta_v}, \tag{18}$$

which for typical noise levels given earlier reduces to

$$\sigma \approx \frac{6.2}{(IA)^{2/3}}. \tag{19}$$

For in-loop sounding with a 300 m loop and 25 A of current, magnetic-field measurements are superior for resistivities of less than 2800 $\Omega \cdot$ m. For a smaller 50 m loop with 10 A of current, this value is lowered to 140 $\Omega \cdot$ m. Thus for the noise level estimates used here, magnetic-field measurements are superior for all but the most resistive areas.

Far-zone sounding.—The term "far zone" applies to sounding where the source-receiver separation or loop size is much greater than the depth of investigation: the induction number $2t/\sigma\mu a^2$ is less than about 0.1.

The relevant expressions for voltage (dB_z/dt) measurements are the early-time response

$$V = \frac{3I}{\sigma a^3} \tag{20a}$$

for the in-loop configuration and

$$V = \frac{3Id\ell}{2\pi\sigma a^4} \tag{20b}$$

for the wire-loop configuration, assuming a receiver moment of 1. The voltage response for far-zone sounding is inversely proportional to the cube of the loop size or the fourth power of the source-receiver separation and directly proportional to resistivity. Since these expressions are not functions of time, they cannot be combined with equation (8) in the same manner as for near-zone sounding. However, the greatest depth of investigation attainable with far-zone sounding is achieved at the latest time at which the far-zone approximation is valid, i.e.,

$$\frac{2t}{\sigma\mu_0 a^2} \approx 0.1. \tag{21}$$

Equating this with the time of departure [equation (8)], it can be shown that the loop size, or transmitter-receiver separation a, must be greater than about three times the depth of investigation. Substituting $a = 3d$ in equations (20a) and (20b), the maximum depths of investigation are

$$d \approx 0.48 \left(\frac{I}{\sigma\eta_v}\right)^{1/3} \tag{22a}$$

for in-loop sounding and

$$d \approx 0.28 \left(\frac{Id\ell}{\sigma\eta_v}\right)^{1/4} \tag{22b}$$

for wire-loop sounding. For values of $a > d$, the depth of investigation varies inversely as a.

The wire-loop configuration is often used for deep sounding (Keller et al., 1984) because large source-receiver separations can be easily deployed and the signals have a relatively small dynamic range. Exploration to a depth of 4 km can be achieved using a source-receiver separation of 12 km, a source length of 4 km, and a transmitter current of 50 A for a 100 $\Omega \cdot$ m earth and 500 A for a 10 $\Omega \cdot$ m earth.

It is not feasible to perform a magnetic-field sounding in the far zone because, as mentioned earlier, it is not possible to measure the slowly decaying field [given by equation (9)] with sufficient accuracy using present technology. In practice the separation between the magnetic-field response of different geoelectric sections cannot be measured until intermediate times are reached.

Intermediate-zone sounding.—In practice a TEM sounding may involve aspects of both near-zone and far-zone soundings if measurements are made over a wide enough time range. A suite of in-loop magnetic-field decay curves for different loop sizes is shown in Figure 9. For a fixed sample time, there is an optimum loop size for which the maximum signal strength is achieved; alternatively, for a particular noise level and transmitter current, there is an optimum loop size for measuring to late time. This occurs in the area of transition between near-zone and far-zone sounding (the intermediate zone) and is delineated by the straight line on the figure. For example, if the noise level or the h_z/I ordinate is set at 0.033, then the optimum loop radius $a = 10$ m, since this enables measurements as late in time as $2t/\sigma\mu = 12$.

The depth of investigation to be used as a constraint when minimizing the transmitted current is derived as follows: From Figure 9, the maximum signal level attainable at any particular sample time is

$$\frac{h_z a}{I} = 0.33, \tag{23a}$$

which is measured at a normalized time

$$\frac{2t}{\sigma\mu} = 0.12\, a^2. \tag{23b}$$

The latest time that measurements can be made is the time at which the signal h_z in equation (23a) decays to the noise level η_B. Combining equations (23a) and (23b), this time is

$$t = 6.5 \times 10^{-3} \sigma \mu_0^3 \left(\frac{I}{\eta_B}\right)^2. \tag{24}$$

Equating t in equation (24) with the time of departure [equation (8)], the maximum depth of investigation achieved is

$$d \approx 1.4 \times 10^{-7} \frac{I}{\eta_B}. \tag{25}$$

Combining equations (23a) and (25) and setting h_z equal to the noise level η_B/μ_0, the loop radius for which the maximum depth of penetration is achieved is

$$a \approx 2.9d, \tag{26a}$$

or, for a square loop of side L,

$$L = a\sqrt{\pi} \approx 5d. \tag{26b}$$

Thus, for a given transmitter current and noise level the maximum depth of exploration, given by equation (25), is achieved by using the loop size given in equation (26). For example, for a noise level of 0.01 nT, a depth of exploration of 100 m is achieved with a 500 m loop size with only 7 mA of current. These calculations show that if transmitter current is the limiting factor, then the maximum depth of investigation is achieved with very large loops sizes.

However, transmitter current is seldom constrained to the low levels shown here. If the current is increased while keeping the loop size fixed, then equation (25) can no longer be used. The depth of investigation must be calculated using the complete expression for the half-space response, as illustrated in Figure 9, and equation (8). The depth of investigation is increased by factors of 3.6, 2.3, and 2.15 for successive factors of 10 increase in the transmitted current. The result of using higher currents is to move down the descending branch of the half-space curve to the region where equation (12) holds, effectively changing the sounding to "near zone."

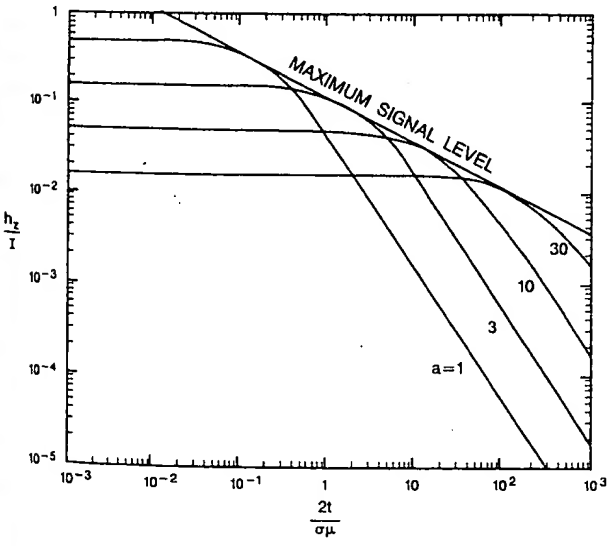

FIG. 9. TEM in-loop magnetic field decay curves for a homogeneous earth. At any fixed sample time t there is an optimum loop radius a, for which the maximum signal level is obtained. This occurs in the intermediate time range, when $2t/\sigma\mu a^2 \approx 0.12$.

For voltage (dB/dt) measurements, the analogous expression to equation (24) for in-loop sounding is

$$t \approx 0.16\sigma^{1/3}\mu_0 \left(\frac{I}{\eta_v}\right)^{2/3}. \tag{27}$$

Equating this with the time of departure [equation (8)], we obtain

$$d \approx 0.55 \left(\frac{I}{\sigma\eta_v}\right)^{1/3}, \tag{28}$$

with

$$a \approx 1.7d. \tag{29a}$$

For a square loop of side L, this becomes

$$L = a\sqrt{\pi} \approx 3d. \tag{29b}$$

As for the near-zone analysis, the optimum parameters for voltage response depend on the resistivity. For exploration to a depth of 200 m, the optimum loop size is 600 m. This can be obtained with a current level of 0.2 mA for a 100 $\Omega \cdot$ m earth and 24 mA for a 1 $\Omega \cdot$ m earth, assuming a noise level of 0.5 nV/m^2. By comparing expressions (25) to (29), it can be seen that voltage measurements are preferable to magnetic-field measurements for shallow intermediate-zone soundings, since a greater depth of investigation can be achieved with the same loop size.

For wire-loop soundings, the depth of investigation obtained under the condition of minimum source moment is

$$d \approx 0.37 \left(\frac{Id\ell}{\sigma\eta_v}\right)^{1/4}, \tag{30}$$

which is obtained with a transmitter-receiver separation

$$a \approx 1.3d. \tag{31}$$

For example, for exploration to a depth of 200 m, the optimum source-receiver separation is 260 m. For a source length of 50 m the transmitter current required is 8.4 mA for a 100 $\Omega \cdot$ m earth and 800 mA for a 1 $\Omega \cdot$ m earth.

By comparing equations (22b) and (30), it can be seen that the depth of investigation obtained with far-zone sounding is inferior to that attainable with intermediate-zone sounding.

Unlike the far-zone case, magnetic-field measurements can be made for grounded-source systems in the intermediate zone. The relevant expressions are

$$d \approx 10^{-4} \left(\frac{Id\ell}{\eta_B}\right)^{1/2} \tag{32}$$

and

$$a \approx 1.7d. \tag{33}$$

The depth of investigation is again independent of conductivity, and the dependence on transmitter moment has in-

creased from 1/4 to 1/2. For the same example given earlier (dipole length 50 m), the depth of investigation of 500 m is achieved by increasing the separation to 850 m and the current to 500 mA. For the same source moment, the depths of investigation attainable with magnetic-field measurements are much greater than for voltage measurements.

With intermediate-zone soundings the depth of investigation is maximized for any given transmitter current (in-loop) or source moment (wire-loop). In practice, intermediate-zone soundings are not often used for the in-loop configuration, since it is more practical to use smaller loop sizes and higher current. In these cases the depth of investigation is greater than the loop size, and the sounding reverts to being "near zone."

COMPARISON OF DIFFERENT METHODS

Although the time of departure or thickness of the overlying section expressed in diffusion depths is reasonably constant for all systems, there are large differences in the maximum depths of investigation achieved in practice when signal and noise levels are considered. Table 1 presents a convenient summary of the expressions derived in this paper for a wide range of source-receiver configurations.

MT is classified as "far zone" because of the great distance of the source. Expressions for CSAMT can be derived in a similar manner to that described for TEM. The depth of investigation of the CSAMT method differs from MT, since signal and noise levels need to be taken into account.

The TEM expressions vary greatly for "near" and "far" zones and differ for voltage (dB/dt) and magnetic-field measurements. The optimum separation and configuration depend on the required depth of exploration and the average resistivity of the overlying section.

The expressions given in Table 1 give the depth of investigation based on *detection* of a buried feature at depth. It is usually necessary to use a larger source moment than that obtained from the table so that measurements can be made at a significantly later time or lower frequency to obtain an unambiguous signature for adequate *resolution*. The amount of additional data required in practice depends on such factors as system accuracy, geologic noise, the dimensions of the target, and its conductivity contrast with the overlying strata. From field experience, however, an additional one-third decade (i.e., a factor of two) of time or frequency is usually adequate.

Applying the one-third decade guideline to the near-zone and intermediate-zone configurations in Table 1 reduces the effective depth of investigation to 71 percent of the values shown. The factor shown in brackets is the increase in source moment required to extend measurements to twice the sample time. A different criterion is applied to near-zone soundings because, as can be seen from Figure 4, the signal level for a homogeneous earth is constant with time and

Table 1. Depth of investigation of various EM sounding methods.

	Near zone $\left(\frac{2t}{\sigma\mu a^2} \geq 5\right)$	Intermediate zone (minimize current)	Far zone $\left(\frac{2t}{\sigma\mu a^2} \leq 0.1;\ a \geq 3d\right)$
MT	N/A	N/A	$750\left(\frac{1}{\sigma f}\right)^{1/2}$
TEM, in-loop, voltage	$0.55\left(\frac{IA}{\sigma\eta_v}\right)^{1/5}$ [5.7]	$0.55\left(\frac{I}{\sigma\eta_v}\right)^{1/3}$ [2.8] when $a = 1.7d$	$0.48\left(\frac{I}{\sigma\eta_v}\right)^{1/3}$ [2] for $a = 3d$
TEM, wire-loop, voltage	$0.48\left(\frac{Iad\ell}{\sigma\eta_v}\right)^{1/5}$ [5.7]	$0.37\left(\frac{Id\ell}{\sigma\eta_v}\right)^{1/4}$ [4] when $a = 1.3d$	$0.28\left(\frac{Id\ell}{\sigma\eta_v}\right)^{1/4}$ [2] for $a = 3d$
TEM, in-loop, magnetic field	$2.8 \times 10^{-3}\left(\frac{IA}{\eta_B}\right)^{1/3}$ [2.8]	$1.4 \times 10^{-7}\frac{I}{\eta_B}$ [1.4] when $a = 2.9d$	can't measure
TEM, wire-loop, magnetic field	$2.4 \times 10^{-3}\left(\frac{Iad\ell}{\eta_B}\right)^{1/3}$ [2.8]	$10^{-4}\left(\frac{Id\ell}{\eta_B}\right)^{1/2}$ [2] when $a = 1.7d$	can't measure

η_v = voltage noise level after stacking (typically 0.5 nV/m^2)
η_B = magnetic-field noise level after stacking (typically 10^{-3} nT)
a = loop radius (in-loop) or transmitter-receiver separation (wire-loop)
A = loop area (in-loop)
I = transmitter current
$d\ell$ = grounded dipole length (wire-loop)

Note: These expressions are based on *detection* of a buried feature at depth. It is usually advisable to use a larger source moment (multiply $Id\ell$ or IA by the factor shown in brackets) to facilitate interpretation (see text).

decreases when a conductive lower layer is detected. The recommendation in this case is to double the source moment.

The range of depths covered in a typical MT and TEM (voltage) sounding is shown in Figure 10. In very conductive regions, the TEM sounding covers several decades of depth; but as the resistivity increases, the depth range narrows. As the loop size is reduced and the resistivity of the ground is increased, the depth range finally decreases to zero; at this point the signal has decayed to the noise level before the first sample time. For this example there is overlap in the depth of investigation obtained with the two methods for resistivities less than 260 Ω · m. Adequate overlap is *essential* for successful implementation of MT static-shift corrections using TEM.

An in-loop TEM (voltage) sounding has the same depth of investigation as MT at a frequency f if its source moment IA is set equal to

$$IA = \left(\frac{2.4 \times 10^6}{\sigma^{3/2}}\right) f^{5/2}, \tag{34}$$

assuming a TEM noise level η_v of 0.5 nV/m^2. For f = 100 Hz and I = 10 A, the depth of investigation in a 1 Ω · m earth is 75 m (using a TEM loop size of 1.5 m), whereas a depth of 2400 m is achieved for a 1000 Ω · m earth (280 m loop size). Similar calculations can be performed for other configurations. It should be mentioned here that it is inadvisable to use very small TEM loops for making MT static-shift corrections because of the possibility of recording anomalous superparamagnetic effects (Spies and Frischknecht, 1989).

EXAMPLE

It is useful to work through a case history of survey design for a typical field problem to illustrate the use of the expressions given in this paper. Consider, for example, that the geologic objective is to map the thickness of volcanics with an average resistivity of 100 Ω · m overlying a 5 Ω · m sedimentary section. The thickness of the volcanics is expected to vary from 0 to 2000 m. A contractor can supply a TEM system capable of in-loop sounding with a transmitter loop size of either 100 m (10 A of current) or 400 m (20 A). The earliest time channel is 50 μs. Moderate noise levels (0.5 nV/m^2) are predicted.

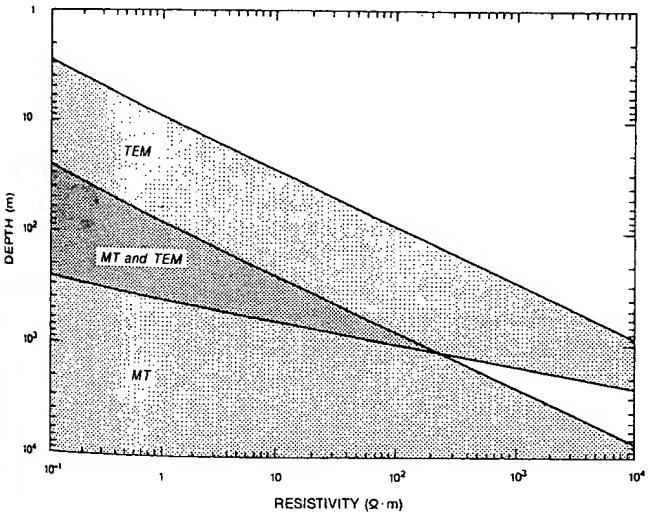

FIG. 10. Comparison of regions of investigation obtained with MT and in-loop TEM (voltage response). For this example the upper MT frequency is 100 Hz, the TEM loop size is 100 m, and the current is 10 A. The depths of investigation of the two methods overlap for resistivities less than 260 Ω · m. To ensure overlap at higher resistivities, it is necessary either to measure at higher MT frequencies or to employ a larger TEM transmitter moment.

Equation (8) sets the limit on the thinnest volcanic cover that can be mapped which, based on the earliest sample time of 50 μs and a resistivity of 100 Ω · m, is calculated to be 90 m (Figure 8 is applicable to this example). Depths shallower than 90 m cannot be resolved with this system.

The maximum depth of investigation is calculated from Table 1 using the near-zone formula, since the depth of investigation is expected to be greater than the loop size. The maximum depth at which the sedimentary basement can be detected is calculated to be 1000 m for the 100 m loop and 2000 m for the 400 m loop. For a confident interpretation, though, these depth estimates should be reduced to 71 percent of these values, i.e., 700 m and 1400 m. The latest sample time at which the signal is above the noise level calculated from equation (8) is 13 ms for the 100 m loop and 53 ms for the 400 m loop. These times are used to choose the appropriate pulse repetition rate. To resolve an interface at a depth of 2000 m, the source moment (area-current product) must be increased by a factor of 5.7, for example, by employing a loop size of 800 m with 30 A of current (a source moment of 1.8 × 10^7 Am^2).

If the system were capable of transmitting into a grounded source, a wire-loop sounding could be made. For far-zone or long-offset sounding the minimum source-receiver separation is 6000 m (a/d = 3). This would require a source moment $Id\ell$ of 13 000 Am, e.g., 26 A transmitted into a 500 m grounded dipole (or 26 000 Am to allow for interpretation of the conductive lower layer). The same source-receiver separation could be used for all depths between 90 m and 2000 m, but unlike the near-zone case, the signal level would not increase for shallower depths of the interface. The smallest possible source moment (4200 Am) is achieved using a separation of 2600 m (intermediate-zone sounding with a/d = 1.3). The source moment should be increased by a factor of 4 to 16 800 Am for interpretation. Larger source moments would be required for smaller separations (near-zone sounding), e.g., 7000 Am for a source-receiver separation $a = 0.45d$ = 900 m. This moment should be increased by a factor of 5.7 to 40 000 Am for interpretation.

The same depth range (90 m to 2000 m) could also be probed with an MT system having a frequency range 7 Hz to 7 kHz (to facilitate interpretation, the 7 Hz value is half that calculated from Table 1).

DISCUSSION

The expressions for the depth of investigation derived for TEM in this paper are based on the detection of a buried half-space. It is logical to question whether the same conclusions would apply to the detection of more general 2-D and 3-D bodies. Newman et al. (1986, 1987) and Newman and Hohmann (1988) published a number of 3-D model

results for the TEM in-loop configuration, and Gunderson et al. (1986) published results for a grounded source. All these models, whether a basement uplift or conductive prism, are first detected under approximately the same thickness of overburden as for the case of the buried half-space. Just as for a buried layer, the exact time at which an interpreter would be confident that a 3-D body is being detected depends on its size and conductivity contrast and is somewhat subjective. For example, Eaton and Hohmann (1989), in a study of 3-D bodies in a layered earth, prefer an estimate of 1.24 diffusion depths. This would have the effect of reducing the depth of investigation given by equation (16) by 11 percent. The exact value chosen will not alter the main conclusions reached in this paper; it will merely result in a slight change in the multiplicative constant.

A basic assumption made in this paper is that the earth can be adequately represented by a 1-D model. This assumption is reasonable for most controlled-source EM soundings in quasi-layered environments. Recent papers (Ranganayaki, 1984; Ingham, 1988) have demonstrated the utility of 1-D interpretation of MT data obtained using rotationally invariant MT parameters, as proposed by Berdichevsky and Dimitriev (1976a). A significant hazard with this approach, however, is the possibility that the data have been corrupted by static effects caused by near-surface inhomogeneities or topography (Berdichevsky and Dimitriev, 1976b; Park, 1985) or large-scale structure which distorts the regional current system (Ranganayaki and Madden, 1980). If, however, the soundings are corrected for static shift using schemes such as those proposed by Rokityansky (1982), Jones (1988), Sternberg et al. (1988), and Bahr (1988) for MT, or by Newman (1989) for TEM sounding, then 1-D inversions will be relatively undistorted, and the relations derived in this paper will give satisfactory results.

Other sources and configurations.—Spies and Frischknecht (1989) show that the time of departure for TEM given by equation (8) is applicable to virtually any source-receiver combination. For grounded dipole-dipole configurations, however, the response curves first need to be adjusted for static shifts caused by dc current flow in the ground.

Similar analyses, relating the depth of investigation to signal and noise levels, can be applied to virtually any EM sounding technique. For example, Keller (1971) calculated similar relationships for a frequency-domain loop-loop system used for sounding in Hawaii. He concluded that the optimum source-receiver separation is twice the depth of investigation, and that the depth of investigation is proportional to the source moment raised to the 2/9 power. Of course the most complete analysis for any EM system is to calculate the EM response over the full range of field parameters, taking into account constraints imposed by signal and noise levels, and measurement accuracy.

Frequency-domain controlled-source methods using a loop-loop (slingram) configuration are often used for shallow sounding, since the operating frequency can be made arbitrarily high and the skin depth reduced accordingly. However, at very high frequencies displacement currents can be significant, thereby complicating interpretation. An alternative approach for shallow sounding is to measure the quadrature response at very low induction numbers, where the penetration of the fields is not limited by the skin effect, but rather by the source-receiver separation r. It can be shown that approximately 75 percent of the response at low induction numbers originates from depths of less than λ (Frischknecht et al., 1989). Most portable terrain conductivity meters are based on this principle.

CONCLUSIONS

The depth of investigation of electromagnetic sounding methods is determined by the frequency or time of measurement, the earth conductivity, and, for controlled-source methods, the source moment and noise levels. The most notable difference among various methods is their sensitivity to the resistivity of the overlying section. The methods considered here, numbered in order of increasing dependence on resistivity, are:

(1) TEM (magnetic field) . . . no dependence
(2) TEM (wire-loop and in-loop, voltage, near zone) . . . depth $\propto \rho^{1/5}$
(3) TEM (wire-loop, voltage, far zone) . . . depth $\propto \rho^{1/4}$
(4) TEM (in loop, voltage, far zone) . . . depth $\propto \rho^{1/3}$
(5) MT . . . depth $\propto \rho^{1/2}$

The MT method, with appropriate static-shift corrections, should be used wherever very large depths of investigation are required. For intermediate depths there is overlap between the MT and TEM methods, which, except for TEM magnetic-field measurements, depends strongly on the earth conductivity.

For a layered-earth section the depth of investigation depends on the average conductivity (defined as the integrated conductance divided by the total thickness) of the overlying section. The average conductivity, calculated as a function of depth, can also be used for estimating an approximate lower depth bound of a layered-earth inversion. The lower bound is the depth which is equal to 1.5 skin depths in the frequency domain, or 1 diffusion depth in the time domain, calculated using the average conductivity at the lowest measurement frequency or latest sample time.

The highest measurement frequency or earliest sample time determines the minimum depth at which individual conductivity variations can be resolved. At depths shallower than approximately 1.5 skin depths or 1 diffusion depth, calculated at the highest measurement frequency or earliest sample time, the response is determined mainly by the average conductivity of the overlying section.

For applications where resolution at very shallow depths is required, such as groundwater, engineering, environmental, and archaeological applications, frequency-domain systems offer the best solution. The earliest sample time in most TEM systems is about 50 μs, which is unsuitable for shallow applications.

ACKNOWLEDGMENTS

This paper evolved over a number of years and has benefited from the input of a large number of people to whom I am grateful. Misac Nabighian, Nigel Edwards, Dwight Eggers, and Frank Morrison contributed early ideas, and Ted Madden, Ulrich Schmucker, Peter Weidelt, Greg Newman, Laszlo Szarka, and anonymous reviewers suggested

later modifications. The paper is published with permission of ARCO Oil and Gas Company.

REFERENCES

Andrieux, P., and Wightman, W. E., 1984, The so-called static corrections in magnetotelluric measurements: 54th Ann. Internat. Mtg., Soc. Expl. Geophys., Expanded abstracts, 43–44.

Bahr, K., 1988, Interpretation of the magnetotelluric impedance tensor: regional induction and local telluric distortion: J. Geophys., **62**, 119–127.

Berdichevsky, M. N., and Dimetriev, V. I., 1976a, Basic principles of interpretation of magnetotelluric sounding curves, *in* Adams, A., Ed., Geoelectrics and geothermal studies: East Central Europe, Soviet Asia: KAPG Geophys. Monogr., Akademiai Kiado, Hungary, 165–221.

——— 1976b, Distortion of magnetic and electric fields by near-surface lateral inhomogeneities: Acta geod. geophys. Mont. Acad. Sci. Hung., **11**, 447–483.

Bostick, F. X., 1977, A simple almost exact method of MT analysis: Workshop on electrical methods in geothermal exploration, U.S. Geol. Surv., contract no. 14080001-8-359.

Chave, A. D., 1984, The Fréchet derivatives of electromagnetic induction: J. Geophys. Res., **89**, 3373–3380.

Constable, S. C., Parker, R. L., and Constable, C. G., 1987, Occam's inversion: A practical algorithm for generating smooth models from electromagnetic data: Geophysics, **52**, 289–300.

Eaton, P. A., and Hohmann, G. W., 1987, An evaluation of electromagnetic methods in the presence of geologic noise: Geophysics, **52**, 1106–1126.

——— 1989, Approximate inversion for transient electromagnetic soundings: Phys. Earth Plan. Int., **53**, issue 3/4.

Edwards, R. N., 1988, A downhole magnetometric resistivity technique for electrical sounding beneath a conductive surface layer: Geophysics, **53**, 528–538.

Fischer, G., Schnegg, P.-A., Peguiron, M., and Le Quang, B. V., 1981, An analytic one-dimensional magnetotelluric inversion scheme: Geophys. J. Roy. Astr. Soc., **67**, 257–278.

Frischknecht, F. C., Labson, V. F., Spies, B. R., and Anderson, W. L., 1989, Profiling methods using small sources, *in* Nabighian, M. N., Ed., Electromagnetic methods in applied geophysics, 2: Soc. Expl. Geophys.

Fullagar, P. K., and Oldenburg, D. W., 1984, Inversion of horizontal loop electromagnetic soundings: Geophysics, **49**, 150–164.

Gamble, T. D., 1983, Simple one-dimensional magnetotelluric inversions: 53rd Ann. Internat. Mtg., Soc. Expl. Geophys., Expanded abstracts, 148–151.

Glasko, V. B., Kulik, N. I., and Tikhonov, A. N., 1972, Determination of the geoelectric cross-section by the regularization method: Zh. vychisl. Mat. mat. Fiz., **12**, 139–149; translated in USSR Computational Mathematics and Mathematical Physics.

Glenn, W. E., Ryu, J., Ward, S. H., Peeples, W. J., and Phillips, R. J., 1973, The inversion of vertical magnetic dipole sounding data: Geophysics, **38**, 1109–1129.

Gómez-Treviño, E., 1987a, Nonlinear integral equations for electromagnetic inverse problems: Geophysics, **52**, 1297–1302.

——— 1987b, A simple sensitivity analysis of time-domain and frequency-domain electromagnetic measurements: Geophysics, **52**, 1418–1423.

Gunderson, B. M., Newman, G. A., and Hohmann, G. W., 1986, Three-dimensional transient electromagnetic response for a grounded wire source: Geophysics, **51**, 2117–2130.

Hoversten, G. M., and Morrison, H. F., 1982, Transient fields of a current loop source above a layered earth: Geophysics, **47**, 1068–1077.

Ingham, M. R., 1988, The use of invariant impedances in magnetotelluric interpretation: Geophys. J., **92**, 165–169.

Jain, S., 1966, A simple method of magnetotelluric interpretation: Geophys. Prosp., **14**, 143–148.

Jones, A. G., 1983, On the equivalence of the "Niblett" and "Bostick" transformations in the magnetotelluric method: J. Geophys., **53**, 72–73.

——— 1988, Static-shift of magnetotelluric data and its removal in a sedimentary basin environment: Geophysics, **53**, 967–978.

Jones, A. G., and Foster, J. H., 1986, An objective real-time data adaptive technique for efficient model resolution improvement in magnetotelluric studies: Geophysics: **51**, 90–97.

Jones, A. G., and Hutton, R., 1979, A multi-station magnetotelluric study in southern Scotland II. Monte-Carlo inversion of the data and its geophysical and tectonic implications: Geophys. J. Roy. Astr. Soc., **56**, 351–368.

Jupp, D. L. B., and Vozoff, K., 1975, Stable iterative methods for inversion of geophysical data: Geophys. J. Roy. Astr. Soc., **42**, 957–967.

Kauahikaua, J., 1981, Interpretation of time-domain electromagnetic sounding in the Calico Hills area, Nevada Test Site, Nye County, Nevada: U. S. Geol. Surv. open-file rep. 81–988.

Keller, G. V., 1971, Natural-field and controlled-source methods in electromagnetic exploration: Geoexpl., **9**, 99–147.

Keller, G. V., Pritchard, J. I., Jacobson, J. J., and Harthill, N., 1984, Megasource time-domain electromagnetic sounding methods: Geophysics, **49**, 993–1009.

Kunetz, G., 1972, Processing and interpretation of magnetotelluric soundings: Geophysics, **37**, 1005–1021.

Larsen, J. C., 1981, A new technique for layered earth magnetotelluric inversion: Geophysics, **46**, 1247–1257.

Lewis, R., and Lee, T., 1978, The transient electric fields above a loop on a halfspace: Bull. Austral. Soc. Expl. Geophys., **9**, 173–177.

Macnae, J., and Lamontagne, Y., 1987, Imaging quasi-layered conductive structures by simple processing of electromagnetic data: Geophysics, **52**, 545–554.

Maxwell, J. C., 1892, A treatise on electricity and magnetism: Clarendon Press.

McCracken, K. G., Oristaglio, M. L., and Hohmann, G. W., 1986, Minimization of noise in electromagnetic exploration systems: Geophysics, **51**, 819–832.

Montgomery, G. E., 1987, Geophysical activity in 1986: The Leading Edge, **6**, no. 8, 25–49.

Mundry, E., and Blohm, E.-K., 1987, Frequency electromagnetic sounding using a vertical magnetic dipole: Geophys. Prosp., **35**, 110–123.

Murakami, Y., 1985, Two representations of the magnetotelluric sounding survey: Geophysics, **50**, 161–164.

Nabetani, S., and Rankin, D., 1969, An inverse method of magnetotelluric analysis of a multilayered earth: Geophysics, **34**, 75–86.

Nabighian, M. N., 1979, Quasi-static transient response of a conductive half-space, an approximate representation: Geophysics, **44**, 1700–1705.

Nabighian, M. N., and Macnae, J. C., 1989. Time-domain electromagnetic prospecting methods, *in* Nabighian, M. N., Ed., Electromagnetic methods in applied geophysics, 2: Soc. Expl. Geophys.

Nekut, A. G., 1987, Direct inversion of time-domain electromagnetic data: Geophysics, **52**, 1431–1435.

Newman, G. A., 1989, Deep transient electromagnetic soundings over near-surface conductors with a grounded source: Geophys. J., **90**, to appear.

Newman, G. A., Anderson, W. L., and Hohmann, G. W., 1987, Interpretation of transient electromagnetic soundings over three-dimensional structures for the central-loop configuration: Geophys. J. Roy. Astr. Soc., **89**, 889–914.

——— 1989, Borehole transient EM response of a three-dimensional body in a conductive earth: Geophysics, **54**, 598–608.

Newman, G. A., Hohmann, G. W., and Anderson, W. L., 1986, Transient electromagnetic response of a three-dimensional body in a layered earth: Geophysics, **51**, 1608–1627.

Newman, G. A., and Hohmann, G. W., 1988, Transient electromagnetic response of high-contrast prisms in a layered earth: Geophysics, **53**, 691–706.

Niblett, E. R., and Sayn-Wittgenstein, C., 1960, Variation of electrical conductivity with depth by the magneto-telluric method: Geophysics, **25**, 998–1008.

Nichols, E. A., Morrison, H. F., and Clarke, J., 1988, Signals and noise in measurements of low-frequency geomagnetic fields: J. Geophys. Res., **93**, 13 743–13 754.

Oldenburg, D. W., 1979, One-dimensional inversion of natural source magnetotelluric observations: Geophysics, **44**, 1218–1244.

——— 1983, Funnel functions in linear and nonlinear appraisal: J. Geophys. Res., **88**, 7387–7398.

Oldenburg, D. W., Whittal, K. P., and Parker, R. L., 1984, Inversion of ocean bottom magnetotelluric data: Revisited: J. Geophys. Res., **89**, 1829–1833.

Oristaglio, M. L., 1982, Diffusion of electromagnetic fields into the earth from a line source of current: Geophysics, **47**, 1585–1592.

Park, S. K., 1985, Distortion of magnetotelluric sounding curves by three-dimensional structures: Geophysics, **50**, 786–797.

Parker, R. L., 1977, The Fréchet derivative for the one-dimensional electromagnetic induction problem: Geophys. J. Roy. Astr. Soc., **49**, 543–547.

——— 1980, The inverse problem of electromagnetic induction: Existence and construction of solutions based on incomplete data: J. Geophys. Res., **85**, 4421–4428.

——— 1982, The existence of a region inaccessible to magnetotelluric sounding: Geophys. J. Roy. Astr. Soc., **68**, 165–170.

Parker, R. L., and Whaler, K. A., 1981, Numerical methods for establishing solutions to the inverse problem of electromagnetic induction: J. Geoph. Res., **86**, 9574–9584.
Price, A. T., 1949, The induction of electric currents in non-uniform thin sheets and shells: Quart. J. Mach. and Appl. Math., **2**, 283–310.
Raiche, A. P., and Spies, B. R., 1981, Coincident-loop transient electromagnetic master curves for interpretation of two-layer earths: Geophysics, **46**, 53–64.
Ranganayaki, R. P., 1984, An interpretative analysis of magnetotelluric data: Geophysics, **49**, 1730–1748.
Ranganayaki, R. P., and Madden, T. R., 1980, Generalized thin sheet analysis in magnetotellurics, an extension of Price's analysis: Geophys. J. Roy. Astr. Soc., **60**, 445–457.
Rokityansky, I. I., 1982, Geoelectric investigation of the earth's crust and mantle: Springer-Verlag.
Schmucker, U., 1970, Anomalies of geomagnetic variations in the southwestern United States: Bull. Scripps Inst. Oceanography, **13**, Univ. of California Press.
——— 1979, Erdmagnetische Variationen und die Elecktrische Leitfähigkeit in tierferen Schichten der Erde: Beiträge zur Geowissenschaft, Sonderheft, **4**, Erich Golze, Göttingen.
——— 1987, Substitute conductors for electromagnetic response estimates: Pure and Appl. Geophys., **125**, 341–367.
Sinha, A. K., 1979, Maxiprobe EMR-16: A new wideband multifrequency E.M. system: Current research, Part B., Geol. Surv. Canada, Paper 79-1B, 23–26.
Spies, B. R., 1988, Local noise prediction filtering for central induction transient electromagnetic sounding: Geophysics, **53**, 1068–1079.
Spies, B. R., and Eggers, D. E., 1986, The use and misuse of apparent resistivity in electromagnetic methods: Geophysics, **51**, 1462–1471.
Spies, B. R., and Frischknecht, F. C., 1989, Electromagnetic sounding, *in* Nabighian, M. N., Ed., Electromagnetic methods in applied geophysics, **2**: Soc. Expl. Geophys.
Srnka, L. J., and Crutchfield, W. Y. II., 1987, Riccati inversion of magnetotelluric data: Geophys. J. Roy. Astr. Soc., **91**, 211–228.
Sternberg, B. K., Washburne, J. C., and Pellerin, L., 1988, Correction for the static shift in magnetotellurics using transient electromagnetic soundings: Geophysics, **53**, 1459–1468.
Szarka, L., and Fischer, G., 1989, Electromagnetic parameters at the surface in terms of the distribution of currents at depth: Geophys. J., **90**, to appear.
Thomson, D. J., and Weaver, J. T., 1975, The complex image approximation for induction in a multi-layered earth: J. Geophys. Res., **80**, 123–129.
Vozoff, K., 1989, The magnetotelluric method, *in* Nabighian, M. N., Ed., Electromagnetic methods in applied geophysics, **2**: Soc. Expl. Geophys.
Wait, J. R., 1969, Electromagnetic fields of sources in lossy media, *in* Antenna theory, part 2, Inter-university electronic series, **7**: McGraw-Hill Book Co.
Wait, J. R., and Spies, K. P., 1969, On the image representation of the quasistatic fields of a line current source above the ground: Canad. J. Phys., **47**, 2731–2733.
Weidelt, P., 1972, The inverse problem of geomagnetic induction: Z. Geophys., **38**, 257–289.
——— 1985, Construction of conductance bounds from magnetotelluric impedances: J. Geophys., **57**, 191–206.
Wilt, M., and Stark, M., 1982, A simple method for calculating apparent resistivity from electromagnetic sounding data: Geophysics, **47**, 1100–1105.

APPENDIX A

CONDUCTIVITY IMAGING—A REVIEW

Most approximate techniques for interpreting EM sounding data are based on direct transformation of observed EM data to inferred conductivity and depth. These techniques, which can be collectively referred to as "conductivity imaging" methods, demonstrate the relationship between skin depth (or diffusion depth) and the effective depth of penetration of EM fields in the earth.

An approximate depth transformation commonly used in magnetotellurics is known as the Bostick transform (Bostick, 1977) or the Niblett Sayn-Wittgenstein transform (Niblett and Sayn-Wittgenstein, 1960). The Bostick transform is based on the asymptotic solutions for a two-layered earth with an infinitely conductive or resistive basement, and the Niblett Sayn-Wittgenstein transform is derived directly from Maxwell's equations; these two transforms can be shown, however, to be equivalent (Jones, 1983). The effective depth of penetration h for these transformations estimated directly from the Cagniard apparent resistivity $\rho_a(\omega)$ is defined by

$$h = \sqrt{\frac{\rho_a(\omega)}{\omega\mu_0}}, \qquad \text{(A-1)}$$

which, for a homogeneous earth, is $1/\sqrt{2}$ or 71 percent of the skin depth given by equation (2). Schmucker (1970, 1979) presents a related approach in which the earth is modeled by a "perfect substitute conductor" at a depth h^*. Weidelt (1972) refers to this depth as the "center of gravity of the in-phase induced current system." The relationship between Bostick's and Schmucker's transformations is discussed by Schmucker (1987); for a homogeneous earth the Schmucker depth is equal to 71 percent of the Bostick-Niblett depth, or 0.5 skin depths. The depth given by equation (A-1) is also used in modified forms of the Bostick-Niblett transform described by Jones and Foster (1986) and Murakami (1985). Estimates for depth of penetration used in other imaging schemes sometimes differ from the figure of 0.71 skin depths used above: Jain (1966) defines his depth of penetration as 0.67 skin depths, and Gamble (1983) uses a figure of 0.62 skin depths. The "depth of penetration" used in this context refers to the depths associated with the corresponding interpreted conductivities, and, as shown earlier, considerably underestimates the actual depth of investigation defined using detection criteria.

Related schemes have also been used for controlled-source FEM data in recent years. Sinha (1979), Wilt and Stark (1982), and Mundry and Blohm (1987) describe approximate interpretation schemes for loop-loop FEM sounding data which are essentially identical to the Bostick-Niblett transform.

Another approach, most commonly applied to TEM data, is based on the calculation of "image depths" in the earth from the inferred diffusion velocity. This originates with Maxwell's (1892) observation that the time-domain fields observed above a thin conductive sheet following a step change in magnetic field are identical to those generated by an image of the source receding with a velocity inversely proportional to the conductance of the sheet. However, the image location for a thin sheet bears no relation to the true current distribution in the sheet. Nabighian (1979) developed an analogous concept for a homogeneous earth and showed that the observed effect of currents diffusing into the earth from a loop source could be approximated by a single current filament moving downward with a velocity

$$v = \frac{2}{\sqrt{\pi\sigma\mu_0 t}},$$

while increasing its horizontal dimension in proportion to the diffusion depth $\sqrt{2\ t/\sigma\mu_0}$. This filament moves downward and outward from the loop in a fashion similar to the actual diffusion currents, but with a higher velocity and at a steeper angle of 47 degrees compared to the 30-degree angle for the locus of the maximum induced currents.

These ideas were used by Macnae and Lamontagne (1987) who developed an approximate conductivity-depth imaging algorithm based on inferred image depths for measurements made both inside and outside a large transmitter loop. They used a combination of 14 discrete images centered at a "reference depth" h to show that the slowness dt/dh of the center of the image distribution was very nearly proportional to the cumulative conductance measured from the surface down to the reference depth and could thus be used to estimate conductivity. Their penetration depth was set equal to 54 percent of the image depth. Nekut (1987) and Eaton and Hohmann (1989) simplified this approach by using a single image to construct the approximate earth section. Eaton and Hohmann found that the best depth estimates were 44 percent of the image depth for a loop or grounded source and vertical-axis receiver and 33 percent for a grounded source and horizontal-axis receiver. A minor adjustment to these depth estimates was made at early times. Nekut found that it was necessary to modify the depth according to the induction number. For large loop sizes (or early times) the depth was set at 71 percent of the image depth, and for small loop sizes (or late times) it was set at 48 percent. These adjustments are not necessary in Macnae and Lamontagne's scheme because the width of their image distribution increases with time.

Frequency-domain solutions using complex images have been used by numerous authors for computing rapid approximate solutions in EM induction studies. Thomson and Weaver (1975) give solutions for an arbitrary magnetic source above a multilayered earth, and Wait and Spies (1969) derive image solutions for a line current source. However, interpretation schemes based on image depths are not widely used for interpreting FEM field data.

APPENDIX B

FRÉCHET DERIVATIVES FOR A PLANE-WAVE SOURCE

The Fréchet derivatives for a homogeneous half-space subject to plane-wave excitation, based on an apparent conductivity definition, are:

$$\Delta\sigma_{a,f}(\omega) = \int_0^\infty 2\ \mathrm{Re}\ (\gamma e^{-2\gamma z})\ \Delta\sigma(z)\ dz$$

for the frequency domain,

$$\Delta\sigma_{a,s}(t) = \int_0^\infty 8\ z\theta^2 e^{-4z^2\theta^2}\ \Delta\sigma(z)\ dz$$

for the time-domain step response, and

$$\Delta\sigma_{a,i}(t) = \int_0^\infty 8\ z\theta^2 e^{-4z^2\theta^2}(3 - 8\ z^2\theta^2)\ \Delta\sigma(z)\ dz$$

for the time-domain impulse response, where $\gamma = \sqrt{i\omega\sigma\mu_0}$, and $\theta = \sqrt{\sigma\mu_0/4t}$, respectively (Gómez-Treviño, 1987b). $\Delta\sigma_a$ is the change in observed apparent conductivity resulting from a small change $\Delta\sigma(z)$ in the conductivity function $\sigma(z)$. The term within the integral sign preceding $\Delta\sigma(z)dz$ is the Fréchet derivative relating the small perturbations $\Delta\sigma(z)$ and $\Delta\sigma_a$. The Fréchet derivatives or sensitivity functions also play the role of weighting functions operating on the conductivity distribution itself, from which the observed responses can be synthesized (Gómez-Treviño, 1987a). Each of the σ_a values represents a distinct weighted average of $\sigma(z)$. The corresponding weighting functions, denoted by $G(z)$, are plotted in Figure B-1.

The observed apparent conductivity is a weighted average of the true conductivity function $\sigma(z)$ from $z = 0$ to a certain depth z_{max}. Although there is theoretically a finite contribution from all depths, the value of z_{max} depends principally on the system accuracy (Weidelt, 1972; Fischer et al., 1981). The step response gives well-behaved localized averages at depth, with the maximum contribution, and hence sensitiv

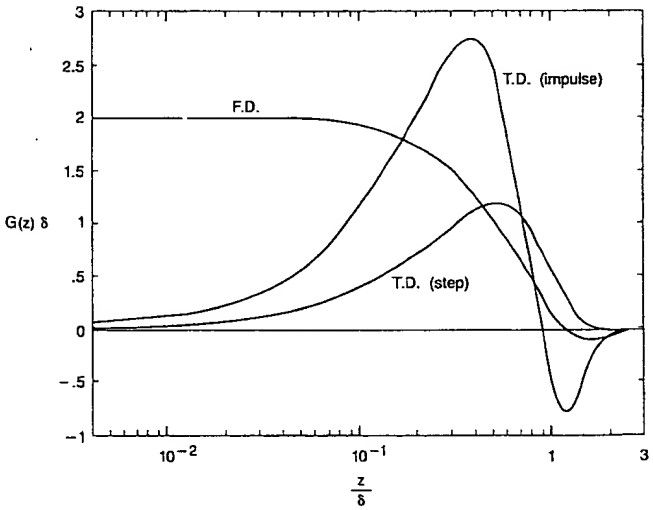

FIG. B-1. Apparent conductivity sensitivity functions for plane-wave exitation of a homogeneous earth in both the frequency domain (F.D.) and time domain (T.D.). Apparent conductivity is a weighted average of the actual earth conductivity from the surface down to a limiting depth controlled by the system accuracy. About 5 percent of the response for F.D. and T.D. (impulse) response, and 1 percent of the step response, originates from depths greater than 1.5 δ. Here δ is the skin depth δ_{FD} in the frequency domain and the diffusion depth δ_{TD} in the time domain (after Gómez-Treviño, 1987b).

ity, at half the diffusion depth δ_{TD} (Figure B-1). Based on the area under the curves, 87 percent of the response originates from depths shallower than δ_{TD}, and 99 percent from depths less than 1.5 δ_{TD}. The frequency-domain and the time-domain impulse responses both have side lobes which are manifested as oscillations in apparent conductivity curves at conductivity discontinuitues. For the time-domain impulse response, the maximum sensitivity is at 0.37 δ_{TD}. There is a positive contribution from depths less than 0.86 δ_{TD}, and a negative contribution from greater depths; 78 percent of the total response originates from depths less than δ_{TD}, and 95 percent from less than 1.5 δ_{TD}. For the frequency-domain case, 95 percent of the response originates from depths shallower than 1.5 δ_{TD}. Since the shape of the sensitivity function depends on the definition used for apparent conductivity (e.g., Spies and Eggers, 1986), caution should be exercised in attaching too much significance to the absolute percentage values given here.

BEST AVAILABLE IMAGES

Defective images within this document are accurate representations of the original documents submitted by the applicant.

Defects in the images include but are not limited to the items checked:

- ☐ BLACK BORDERS
- ☐ IMAGE CUT OFF AT TOP, BOTTOM OR SIDES
- ☐ FADED TEXT OR DRAWING
- ☐ BLURED OR ILLEGIBLE TEXT OR DRAWING
- ☐ SKEWED/SLANTED IMAGES
- ☐ COLORED OR BLACK AND WHITE PHOTOGRAPHS
- ☐ GRAY SCALE DOCUMENTS
- ☐ LINES OR MARKS ON ORIGINAL DOCUMENT
- ☐ REPERENCE(S) OR EXHIBIT(S) SUBMITTED ARE POOR QUALITY
- ☐ OTHER: _____

IMAGES ARE BEST AVAILABLE COPY.
As rescanning documents *will not* correct images problems checked, please do not report the problems to the IFW Image Problem Mailbox